Chemical Science

ROYAL SOCIETY OF CHEMISTRY

EDGE ARTICLE

View Article Online
View Journal

Cite this: DOI: 10.1039/d6sc03261c

All publication charges for this article have been paid for by the Royal Society of Chemistry

Electronegatively substituted adamantyl units accelerate chemiexcitation of 1,2-dioxetane luminophores while preserving chemical stability

Thomas Leirikh,[a] Noa Naama,[a] Dingxing Wang,[a] Liang Ge,[a] Julian Ihssen,[b] Mario Hupfeld,[b] Phil S. Baran[c] and Doron Shabat *[a]

Chemiluminescent probes offer exceptional sensitivity for bioanalytical applications by generating light without external excitation, thereby eliminating background interference. Among these, phenoxy-1,2-dioxetane luminophores are widely used; however, enhancing chemiexcitation rates typically comes at the cost of reduced chemical stability. Here, we present a rational design strategy that overcomes this limitation through the incorporation of electronegatively substituted adamantyl units into the dioxetane scaffold. We show that introducing electron-withdrawing functionality, specifically a lactone-adamantyl moiety, significantly accelerates chemiexcitation kinetics while preserving the inherent stability of the adamantyl framework. These modified luminophores exhibit a transition from prolonged glow-type emission to rapid flash-type chemiluminescence, increasing photon flux without diminishing total light output. As a result, probes incorporating electronegative adamantyl groups demonstrate substantially improved analytical performance. In enzymatic assays, these probes generate faster signal buildup and markedly enhanced signal-to-noise (S/N) ratios compared to classical analogues. This enhancement arises from both accelerated chemiexcitation and reduced background signal due to faster decomposition of residual emissive species. Importantly, stability studies confirm that these structural modifications do not compromise probe integrity under physiological conditions. The practical advantage of this design is clearly demonstrated in bacterial detection assays. Probes bearing the lactone-adamantyl unit achieve signal-to-noise values up to 190-fold higher than those obtained with the corresponding non-substituted adamantyl probes, while maintaining chemical stability under physiological conditions, all within the first minute of measurement. This work establishes substituted adamantyl units as a powerful structural motif for designing next-generation, highly sensitive chemiluminescent tools for rapid diagnostics, bioimaging, and environmental sensing.

Received 19th April 2026
Accepted 13th May 2026

DOI: 10.1039/d6sc03261c

rsc.li/chemical-science

Introduction

During the past three decades, chemiluminescent probes have become indispensable molecular tools across numerous scientific and diagnostic applications.[1–7] In contrast to fluorescence, where light emission requires external excitation, chemiluminescence generates light directly from a chemical reaction. This inherent mechanism confers exceptional sensitivity by eliminating background signals caused by autofluorescence and light scattering. The advent of modular, turn-on chemiluminescent probes dates back to 1987, following the discovery of triggerable phenoxy-1,2-dioxetanes (Fig. 1A).[8–10] In these systems, the phenol group is protected with a substrate tailored to a specific enzyme, allowing for selective detection of enzymatic activity. Once the protecting group is removed by the target enzyme, the chemiexcitation process proceeds, yielding an excited benzoate that decays to its ground state through the emission of light. However, the excited intermediate, formed during the chemiexcitation of Schaap's dioxetane, is quenched by water molecules. Thus, an assay based on this probe requires the presence of an amphiphilic micellar component and a fluorescent dye amplifier. About nine years ago, our group discovered that the incorporation of an acrylate substituent at the *ortho* position of a phenoxy-adamantyl-1,2-dioxetane prevents water-mediated quenching of the excited intermediate and amplifies the light-emission intensity of the chemiluminescent luminophore by up to 3000-fold (Fig. 1B).[11] Importantly, this development enabled the use of chemiluminescent probes as a single component with no required additives.[12–30] Several research groups worldwide have leveraged this discovery to develop novel chemiluminescent probes for a wide range of biological applications.[31–37]

[a]School of Chemistry, Faculty of Exact Sciences, Tel-Aviv University, Tel Aviv 69978, Israel. E-mail: chdoron@tauex.tau.ac.il
[b]Nemis Technologies AG, Zurich, Switzerland
[c]Department of Chemistry, Scripps Research, La Jolla, CA 92037, USA

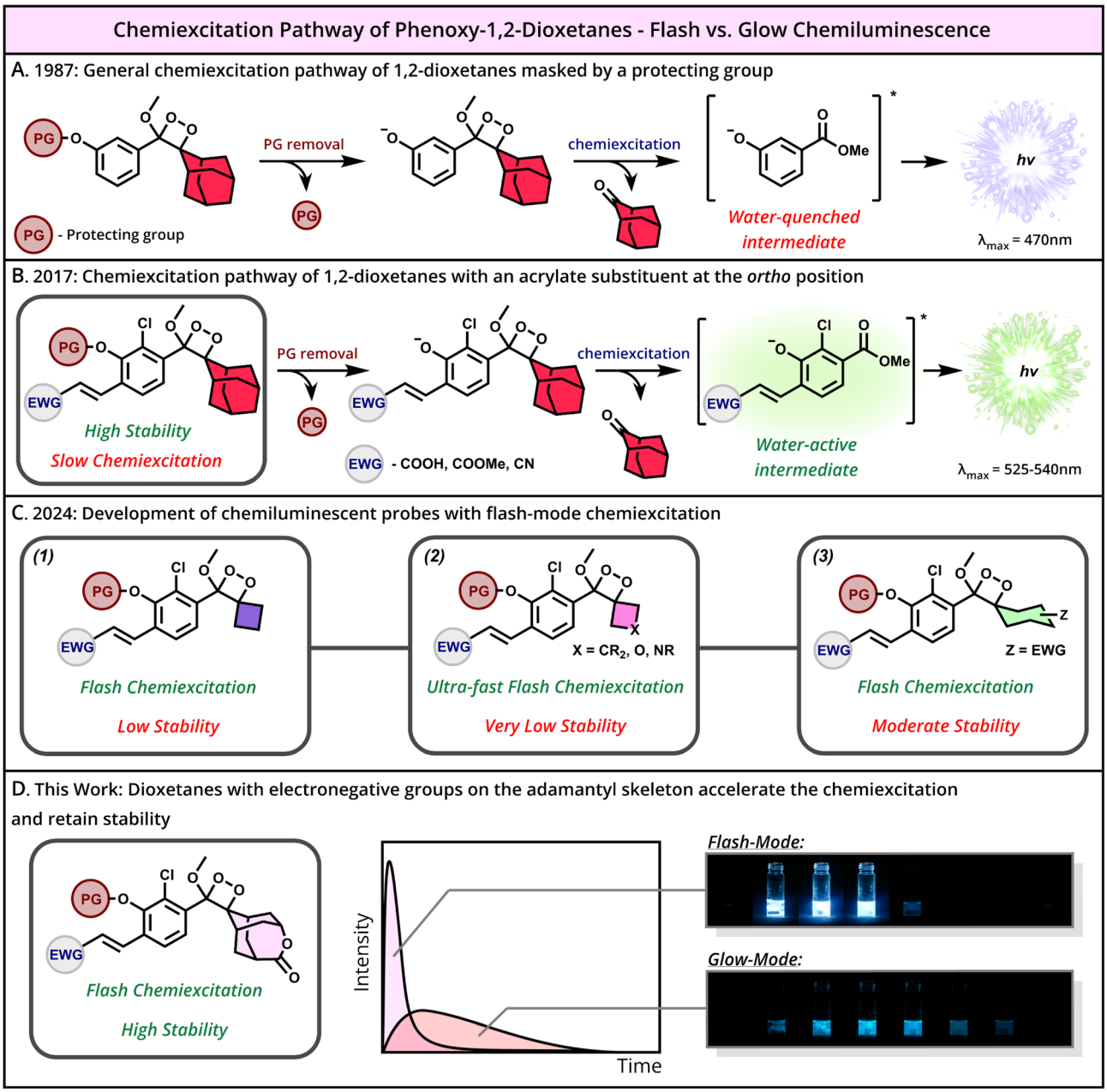

Fig. 1 (A) General chemiexcitation pathway of 1,2-dioxetanes. (B) Activation and chemiexcitation pathway of 1,2-dioxetanes with *ortho* acrylate substituent. (C) Development path of chemiluminescent probes with flash-mode of chemiexcitation. (D) This work: 1,2-dioxetanes bearing electron-withdrawing groups on the adamantyl scaffold accelerate the chemiexcitation and retain the chemical stability. Flash-mode *vs.* glow-mode of chemiexcitation – schematic representation.

Depending on the rate of chemiexcitation, the emission may manifest as a prolonged, low-intensity glow or as a rapid, high-intensity flash. Assays that rely on flash-type chemiluminescence generally offer higher detection sensitivity than those employing glow-type reactions. Recently, our group discovered that introducing spiro-strain into 1,2-dioxetanes markedly increases their chemiexcitation rate, and thereby effectively converts glow-type chemiluminescence into flash-type emission (Fig. 1C1).[38,39] Furthermore, we found that the incorporation of heteroatoms or inductive electron-withdrawing groups on strained four-member or non-strained six-member rings of dioxetanes exhibits even faster chemiexcitation rates (Fig. 1C2 and 1C3).[40,41]

However, further analysis of the structure–activity relationships revealed that both spiro-strained four-membered rings and non-strained substituted six-membered rings severely compromise the chemical stability of the resulting dioxetanes when compared to 1,2-dioxetanes bearing an adamantyl group. In order to obtain dioxetane luminophores that exhibit both accelerated chemiexcitation and high chemical stability, we

sought to introduce an electronegative functionality while retaining the adamantyl structural motif. This dual effect can be achieved by designing adamantyl derivatives bearing electronegative heteroatoms or inductive electron-withdrawing groups. Here we report the design synthesis of dioxetane luminophores equipped with adamantyl units bearing electronegative functional groups (Fig. 1D). These new dioxetane lumiphores exhibit fast chemiexcitation, high chemical stability, improved water solubility, and better detection sensitivity.

Results and discussion

To assess the impact of electronegative adamantyl units on the chemiexcitation rate of phenoxy dioxetanes, we first attempted to induce light emission using tetrabutylammonium fluoride (TBAF) and simple *tert*-butyldimethyl silyl (TBS)-protected phenols (Fig. 2A). Therefore, we synthesized four TBS-protected phenoxy dioxetanes bearing different adamantyl derivatives (Fig. 2B). The first compound, Diox 1, is the classical unsubstituted dioxetane containing a non-functionalized adamantyl group. Diox 2 features an adamantyl moiety in which one carbon atom is oxidized to a carbonyl group. Diox 3 contains an adamantyl derivative further oxidized to a lactone. Finally, Diox 4 incorporates an adamantyl carbonyl derivative in which the two α-positions adjacent to the carbonyl are substituted with ethyl carboxylate ester functionalities.

The four TBS-protected phenoxy-dioxetanes were incubated in DMSO, and their chemiexcitation rates were measured upon the addition of TBAF. The relative chemiexcitation rates were determined from plots of the total light emission $t_{1/2}$ values, as shown in Fig. 2C1. All three dioxetanes containing electronegative adamantyl units (Diox 2, Diox 3, and Diox 4) exhibited substantially faster chemiexcitation rates compared to Diox 1. The relative rate values are summarized in Fig. 2C2, showing that the chemiexcitation rates of Diox 2, Diox 3, and Diox 4 were 13.2, 8.8, and 7.6-fold higher than that of Diox 1, respectively. Fig. 2C3 presents images of the reaction vials captured at selected time intervals over a 5 second period. Diox 1 displayed relatively slow and prolonged light emission lasting well beyond

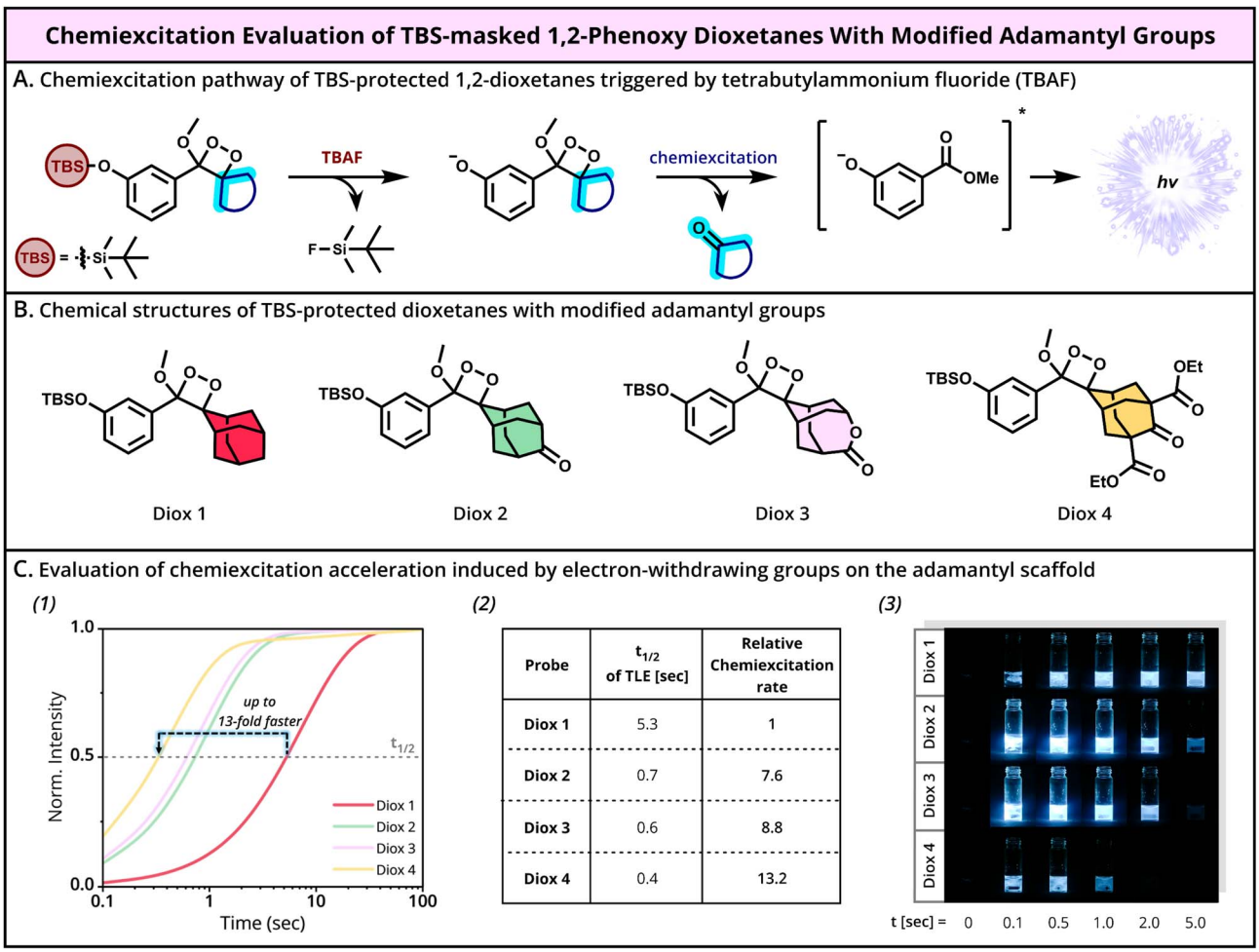

Fig. 2 (A) General activation pathway of TBS-protected 1,2-phenoxy dioxetanes with TBAF. (B) Chemical structures of TBS-protected dioxetanes. (C) Chemiluminescent properties evaluation. (1) Normalized intensity of total light emission of the dioxetanes [10 nM] in DMSO in the presence of TBAF [10 mM] (logarithmic time scale). (2) Half-life values ($t_{1/2}$) of emission, defined as the time by which half of the light is emitted, and relative values of chemiexcitation rate. (3) Visual demonstration of Diox 1–4 activation [500 μM] in DMSO in the presence of TBAF [20 mM].

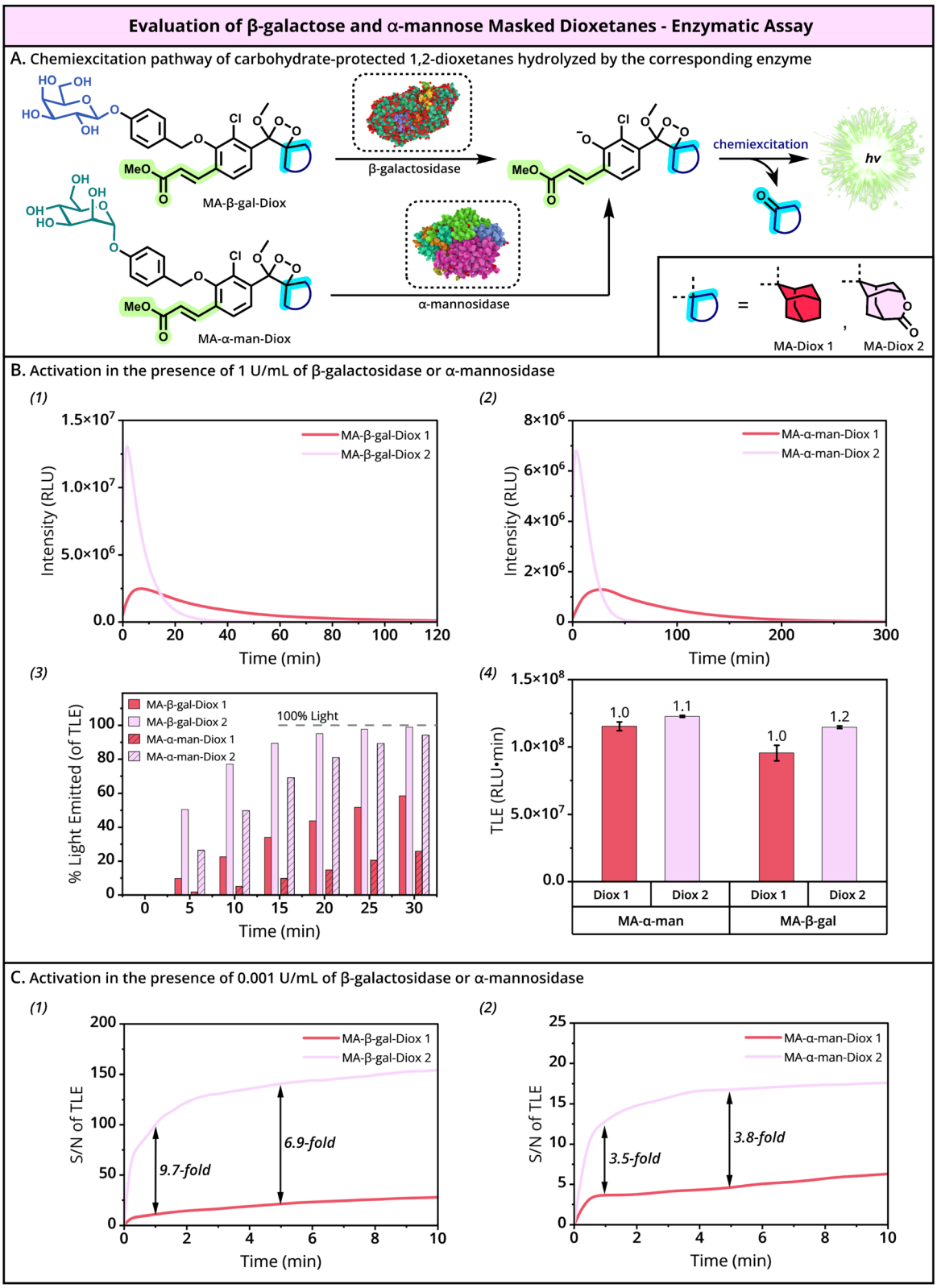

Fig. 3 (A) Chemiluminescent activation pathway of *ortho*-methyl acrylate 1,2-dioxetanes bearing β-galactosidase or α-mannosidase responsive triggers. (B) Activation of the probes [10 μM] in the presence of the corresponding enzyme [1 U mL^{-1}] in PBS 7.4 with 10% ACN at 37 °C. (1) Chemiluminescent kinetic profiles of MA-β-gal-Diox 1 and 2 activated by β-galactosidase. (2) Chemiluminescent kinetic profiles of MA-α-man-Diox 1 and 2 activated by α-mannosidase. (3) Normalized total light emission (in %) of the total light emitted in intervals of 5 min of probes MA-β-gal-Diox 1, MA-β-gal-Diox 2, MA-α-man-Diox 1, and MA-α-man-Diox 2. (4) Total light emission (in relative luminescence units times minutes) of probes MA-β-gal-Diox 1, MA-β-gal-Diox 2, MA-α-man-Diox 1, and MA-α-man-Diox 2 with relative values as column labels. (C) Saturation kinetics – activation of the probes [10 μM] in the presence of the corresponding enzyme [0.001 U mL^{-1}] in PBS 7.4 with 10% ACN at 37 °C. (1) Signal-to-noise of total light emission as a function of time of probes MA-β-gal-Diox 1 and MA-β-gal-Diox 2. (2) Signal-to-noise of total light emission as a function of time of probes MA-α-man-Diox 1 and MA-α-man-Diox 2.

5 seconds, whereas Diox 2, Diox 3, and Diox 4 showed markedly faster chemiexcitation accompanied by shorter emission durations. Videos demonstrating the effect of the modified adamantyl groups on chemiexcitation are included in the SI (Video S1 and S2).

Although Diox 4 exhibits a faster chemiexcitation rate than Diox 2 and Diox 3, its total light emission was substantially lower (Fig. S1). In contrast, both Diox 2 and Diox 3 produced total light emissions comparable to Diox 1, with Diox 3 displaying a slightly faster chemiexcitation rate. These observations prompted further evaluations of probes incorporating adamantyl units with electronegative groups, using the adamantyl-lactone unit of Diox 3 as the structural basis.

Therefore, we next sought to evaluate how the adamantyl-lactone unit, relative to the classic adamantyl group, affects the light emission of chemiluminescent probes designed to function under physiological conditions. As noted in the introduction, phenoxy-1,2-dioxetanes bearing an acrylate substituent are highly emissive luminophores under aqueous conditions. Therefore, two new probes incorporating an adamantyl-lactone scaffold were synthesized (Fig. 3A: MA-β-gal-Diox 2 and MA-α-man-Diox 2). Each probe consists of a methyl acrylate-substituted phenoxy-dioxetane luminophore linked to a glycosidic triggering substrate, one designed for activation by β-galactosidase and the other by α-mannosidase. In addition, two analogous probes featuring a classic adamantyl unit instead of the adamantyl-lactone, equipped with β-galactose and α-mannose triggering substrates, were also prepared (Fig. 3A: MA-β-gal-Diox 1 and MA-α-man-Diox 1).

Probes MA-β-gal-Diox 1 and MA-β-gal-Diox 2 were incubated in PBS (pH 7.4) in the presence of β-galactosidase, while probes MA-α-man-Diox 1 and MA-α-man-Diox 2 were incubated with α-mannosidase (high enzyme concentration). The light-emission profiles of each probe pair were recorded and are presented in Fig. 3B. As expected, the light-emission profiles of the probes containing the adamantyl-lactone (MA-β-gal-Diox 2 and MA-α-man-Diox 2) unit were markedly faster than those of the probes with the classic adamantyl unit (MA-β-gal-Diox 1 and MA-α-man-Diox 1), whose emission persisted over a much longer time interval (Fig. 3B1 and 3B2).

Fig. 3B3 shows the percentage of total light emitted at 5 minute intervals. For example, probe MA-α-man-Diox 2 emitted 50% of its total light within 10 minutes, whereas probe MA-α-man-Diox 1 emitted less than 10% during the same time period. Similarly, probe MA-β-gal-Diox 2 emitted all of its light within 30 minutes, while probe MA-β-gal-Diox 1 emitted less than 60% over that time. The total light emission of all four probes, representing their chemiluminescence quantum yield, was nearly identical, with the adamantyl-lactone probes (MA-β-gal-Diox 2 and MA-α-man-Diox 2) exhibiting values 10–20% higher than the classic adamantyl probes (Fig. 3B4).

The chemiexcitation acceleration effect observed for phenoxy-1,2-dioxetanes containing the adamantyl-lactone suggests that probes MA-β-gal-Diox-2 and MA-α-man-Diox-2, are expected to exhibit higher detection sensitivity compared to their classic adamantyl counterparts. To evaluate this effect, the light emission signals of the probes were then measured under saturation kinetics conditions (low enzyme concentration). Under such conditions, the generated signal is gradually increased to a plateau level (Fig. S2, 3C1 and 3C2). The S/N values measured for probes MA-β-gal-Diox-2 and MA-α-man-Diox-2, over 10 min, were substantially higher than the S/N values measured for the control probes, MA-β-gal-Diox-1 and MA-α-man-Diox-1 (after 1 min, 9.7-fold and 3.5-fold, respectively). These results confirm the enhanced detection sensitivity resulting from the chemiexcitation-acceleration effect of phenoxy-1,2-dioxetane luminophores bearing adamantyl units with electronegative heteroatoms or functional groups.

We recently reported that phenylamine-1,2-dioxetanes are effective chemiluminescent luminophores for aqueous applications.[42] These luminophores exhibit high light-emission intensity as single-component probes and do not require the *ortho*-acrylate substituent that is necessary for their phenoxy-1,2-dioxetane counterparts. Unlike phenoxy-1,2-dioxetanes, the chemiexcitation of phenylamine-1,2-dioxetanes is initiated by electron transfer from the nitrogen lone pair of the amine group. Because this lone pair has a significantly lower charge density than that of the phenolate ion, the chemiexcitation process is relatively slow. Consequently, this limitation reduces the signal-to-noise (S/N) ratio achievable with this new class of chemiluminescent luminophores.

To improve the detection sensitivity of phenylamine-1,2-dioxetanes, we next sought to evaluate the effect of the adamantyl-lactone on the chemiexcitation of these luminophores. The general chemiexcitation pathway of *N*-methyl-phenylamine-1,2-dioxetane probes aimed for the detection of β-gal activity is presented in Fig. 4A. Probe β-gal-NHMe-Diox 2, incorporating an adamantyl-lactone unit, was synthesized, and its light-emission properties were compared with those of probe β-gal-NHMe-Diox 1, which contains a conventional adamantyl moiety (Fig. 4B).

The two probes (β-gal-NHMe-Diox 1and β-gal-NHMe-Diox 2) were incubated in PBS (pH 7.4) in the presence of β-galactosidase (high enzyme concentration), and the light-emission profiles were recorded and are presented in Fig. 4C1. As expected, the light-emission profile of the probe containing the adamantyl-lactone unit (β-gal-NHMe-Diox 2) was markedly faster than that of the probe with the classic adamantyl unit (β-gal-NHMe-Diox 1), whose emission persisted over a much longer time interval. The total light emission produced by the two probes was similar (Fig. 4C1, inset).

The light emission signals of the probes were then measured under saturation kinetics conditions (low enzyme concentration). The S/N value measured for probe β-gal-NHMe-Diox 2, over 10 min, was substantially higher than the S/N values measured for probe β-gal-NHMe-Diox 1 (after 1 min, 3.8-fold and after 5 min, 3.0-fold, respectively).

These results clearly demonstrate the enhanced detection sensitivity achieved through the chemiexcitation-acceleration effect of phenylamine-1,2-dioxetane luminophores bearing a lactone-adamantyl unit, particularly when compared to their classic, non-substituted adamantyl counterparts. This improvement can be attributed to the unique electronic and structural contributions of the lactone-adamantyl moiety,

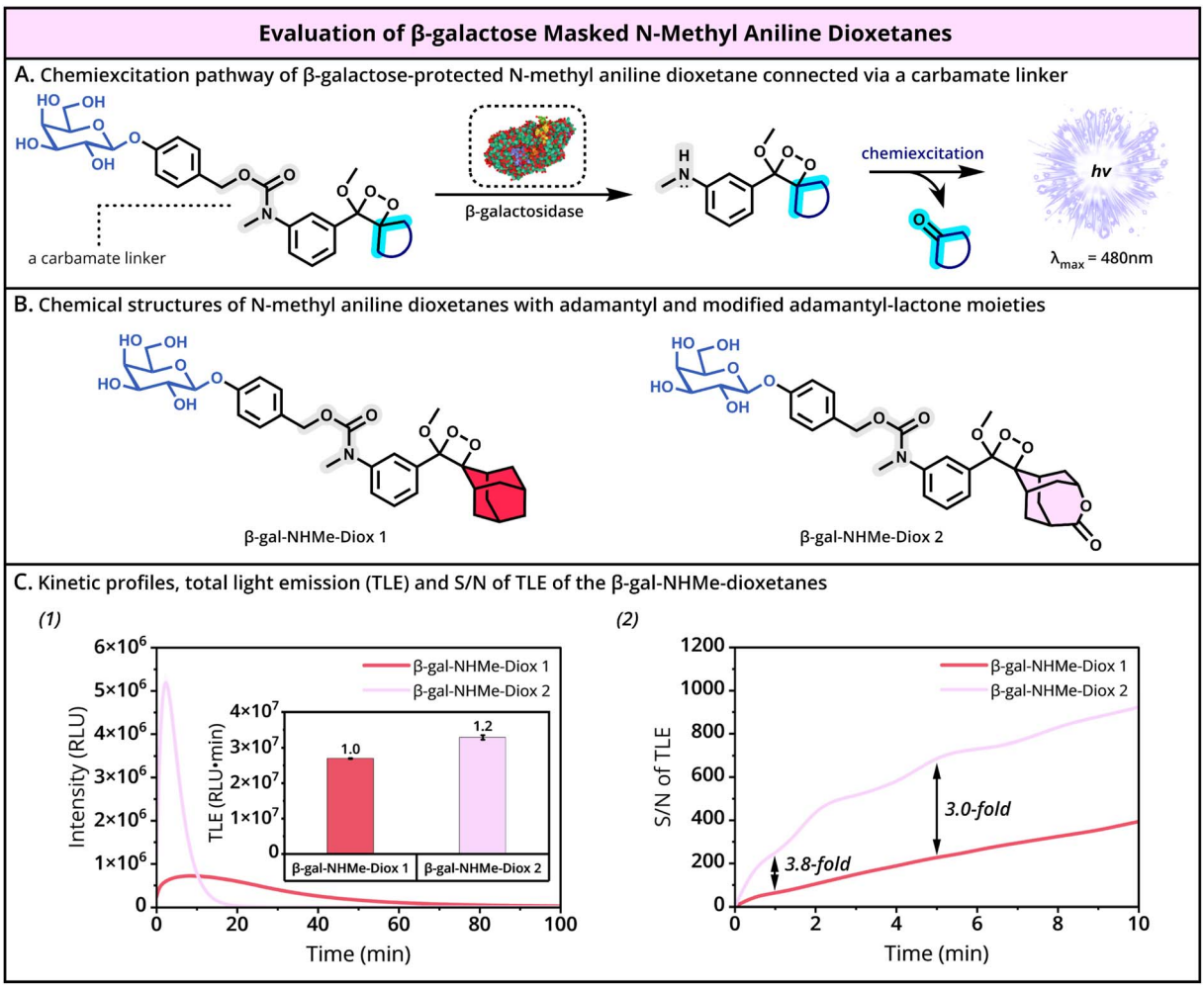

Fig. 4 (A) Chemiluminescent activation pathway of NMe-carbamate-linked 1,2-dioxetane bearing a β-galactosidase-responsive trigger. (B) Chemical structures of NMe-carbamate-linked 1,2-dioxetanes with a β-galactosidase-responsive trigger. (C) (1) Activation of the probes [10 μM] in the presence of β-galactosidase [1 U mL^{-1}] in PBS 7.4 with 10% ACN at 37 °C with TLE-bar inset. (2) Signal-to-noise of total light emission as a function of time of probes NHMe-Diox 1 and NHMe-Diox 2[10 μM] in the presence of β-galactosidase [0.01 U mL^{-1}] in PBS 7.4 with 10% ACN at 37 °C.

which appears to facilitate more efficient energy transfer and promote faster decomposition of the dioxetane intermediate. As a result, the system exhibits a stronger and more rapid luminescent response, enabling more precise and sensitive detection of target analytes. Moreover, these findings highlight the importance of rational molecular design in optimizing chemiluminescent probes, suggesting that strategic substitution on the adamantyl framework can significantly influence both the kinetics and intensity of light emission. Collectively, this underscores the potential of such modified luminophores for advanced analytical and bioimaging applications, where high sensitivity and rapid signal generation are critical.

Finally, we aimed to demonstrate the practical advantage of chemiexcitation acceleration within a biologically relevant assay. The enhanced chemiluminescence rate observed for 1,2-dioxetane luminophores bearing a lactone-adamantyl unit prompted us to investigate whether this improvement could be translated into increased detection sensitivity for bacterial cells expressing enzymes that activate the corresponding chemiluminescent probes (Fig. 5A). Two bacterial strains were employed in this assay: *E. coli* DSM 5923, which expresses β-galactosidase, and *E. thailandicus* NEMIS 502, which expresses α-mannosidase. *E. coli* DSM 5923 was incubated with the probes MA-β-gal-Diox-1 and MA-β-gal-Diox-2, and the resulting light emission was monitored over 10 minutes (Fig. 5B1). Although MA-β-gal-Diox-2, bearing a lactone-adamantyl unit, exhibited only an approximately twofold increase in signal intensity compared to MA-β-gal-Diox-1, which contains a non-substituted adamantyl group, the corresponding signal-to-noise (S/N) ratios were markedly higher (Fig. 5B2). Remarkably, within only 0.5 min of incubation, probe MA-β-gal-Diox-2 reached a maximum S/N value 190 times higher than that of probe MA-β-gal-Diox-1. Although this difference decreased slightly over the subsequent measurement intervals, it remained substantially higher for the lactone-adamantyl probe than for its non-substituted counterpart. A similar trend was observed for *E. thailandicus*

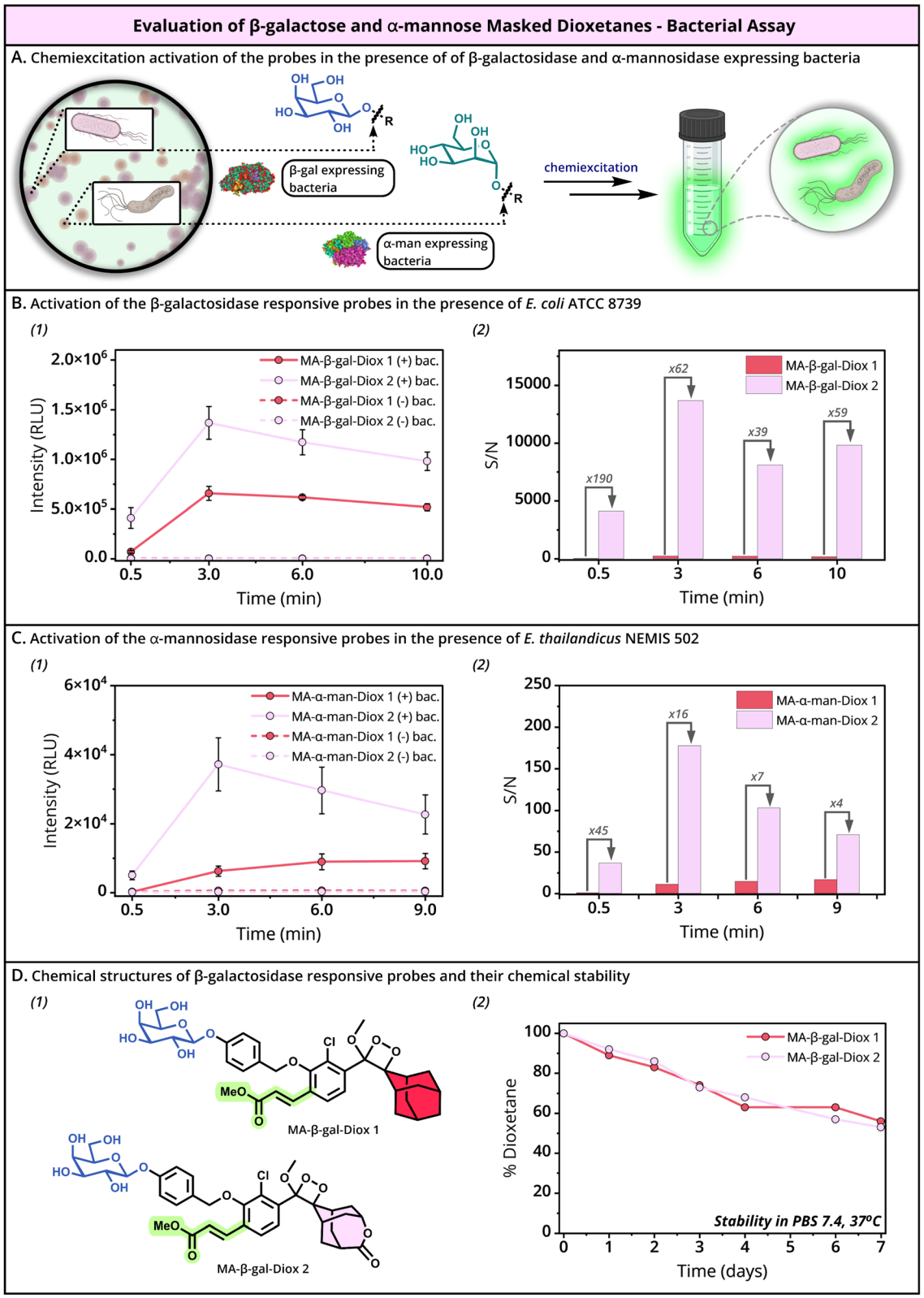

Fig. 5 (A) Illustration of chemiluminescent activation of β-galactose and α-mannose masked 1,2-dioxetanes in the presence of β-galactosidase and α-mannosidase expressing bacteria. (B) (1) Activation of the probes [20 μM] in the presence of *E. coli* ATCC 8739 (10^6 cells) in PBS 7.4, at 37 °C. (2) Signal-to-noise of each β-galactosidase probe at various time points. (C) (1) Activation of the probes [20 μM] in the presence of *E. thailandicus* NEMIS 502 (10^9 cells) in PBS 7.4, at 37 °C. (2) Signal-to-noise of each α-mannosidase probe at various time points. (D) (1) Chemical structures of the probes with β-galactose trigger. (2) Chemical stability evaluation in PBS 7.4 at 37 °C determined by RP-HPLC assay.

NEMIS 502, which was incubated with probes MA-α-man-Diox-1 and MA-α-man-Diox-2 under the same conditions (Fig. 5C1). In this case, a maximum S/N ratio of 45 times higher was also reached at 0.5 minutes post-incubation (Fig. 5C2). While the ratio gradually declined over the following intervals, it consistently remained higher for the lactone-adamantyl probe compared to the non-substituted adamantyl analogue.

The accelerated chemiexcitation rate of probes bearing a lactone-adamantyl unit raises the question of whether this modification compromises their chemical stability relative to their non-substituted adamantyl analogues (Fig. 5D1). To address this, we evaluated the chemical stability of probe MA-β-gal-Diox-1 in comparison with MA-β-gal-Diox-2. Both probes were incubated in PBS (pH 7.4) at 37 °C, and their degradation was monitored over a 7 day period using analytical RP-HPLC (Fig. 5D2). Both probes exhibited gradual and limited degradation over the course of the experiment, with no significant differences observed between them. These results indicate that replacing the conventional adamantyl unit with a lactone-adamantyl moiety does not adversely affect the chemical stability of the 1,2-dioxetane probe. It should be noted that the standard measurement interval for chemiluminescence assays typically ranges from 1 to 5 minutes. Therefore, the slow degradation observed over the extended incubation period is unlikely to have any practical impact on assay performance.

These results clearly demonstrate that accelerating chemiexcitation through the incorporation of a lactone-adamantyl unit significantly enhances the performance of phenoxy-1,2-dioxetane probes in practical biological assays, yielding markedly improved signal-to-noise ratios and rapid detection of enzyme-expressing bacteria, while maintaining chemical stability under physiological conditions.

Flash-type chemiluminescence probes, with chemiexcitation acceleration, generate more intense light emission signals in comparison to glow-type probes, primarily because they produce a higher number of photons within a given time interval. This effect not only enhances the probe's emission signal but also significantly reduces background noise, thereby resulting in a higher signal-to-noise (S/N) ratio. The background noise signal primarily arises from small amounts of probe hydrolysis, occurring during purification by RP-HPLC. This hydrolysis generates trace quantities of phenol-dioxetane, which can undergo chemiexcitation and thus contribute to the observed background signal. To address this issue, phenoxy-1,2-dioxetane probes are typically preincubated in the assay solution for 30 minutes prior to measurement. During this period, trace amounts of phenol-dioxetane decompose *via* the chemiexcitation process. However, if the chemiexcitation rate is slow, a portion of the phenol-dioxetane may persist even after the preincubation step. The phenol-dioxetane degradation product of phenoxy-1,2-dioxetane probes bearing a lactone-adamantyl unit undergoes significantly faster decomposition compared to the corresponding classic adamantyl analogue, thereby resulting in a substantially lower background signal and higher S/N ratio. These reflections can explain why probes MA-β-gal-Diox-2 and MA-α-man-Diox-2 exhibit considerably higher S/N values compared to probes MA-β-gal-Diox-1 and MA-α-man-Diox-1.

The effect of electron-withdrawing units on the chemiexcitation of phenoxy-dioxetane substituted with a six-membered ring was recently reported by our group.[40] In this study, we performed comprehensive DFT calculations that strongly support the experimentally observed acceleration of chemiexcitation induced by electron-withdrawing substituents. Specifically, we found that incorporation of inductively electron-withdrawing groups containing heteroatoms lowers the energy barrier for O–O peroxide bond cleavage, the rate-determining step that initiates chemiexcitation. Similarly, in this work, the incorporation of electron-withdrawing motives on the adamantyl scaffold lowers the activation barrier for the rate-limiting step of chemiexcitation.

Higher signal-to-noise (S/N) ratios directly translate into improved limits of detection (LOD), as a stronger signal relative to background noise enables more reliable identification of low-abundance targets. In our previous studies, we demonstrated that phenoxy-1,2-dioxetane probes exhibiting accelerated chemiexcitation consistently produce elevated S/N values, which in turn enhance detection sensitivity.[38–40,43] This effect was particularly evident in the detection of β-galactosidase activity in *E. coli* assays, where probes with faster chemiexcitation enabled clearer signal discrimination at lower analyte concentrations. Consequently, these probes achieved significantly lower LOD values compared to their slower-emitting counterparts, underscoring the critical role of chemiexcitation kinetics in improving analytical performance.

Conclusions

In summary, we report the rational design of 1,2-dioxetane luminophores incorporating electronegatively substituted adamantyl units, which successfully combine accelerated chemiexcitation with preserved chemical stability. By introducing a lactone-adamantyl moiety, we achieved a substantial increase in chemiexcitation rates without compromising the intrinsic robustness of the adamantyl scaffold. This design overcomes a key limitation observed in previous strategies, where enhanced reactivity was often accompanied by reduced stability. The modified luminophores exhibit flash-type chemiluminescence characterized by rapid and intense light emission, while maintaining total light output comparable to classical systems. Importantly, this acceleration translates directly into improved analytical performance. In both enzymatic assays and bacterial detection models, probes bearing the lactone-adamantyl unit consistently produced markedly higher signal-to-noise ratios, enabling faster and more sensitive detection. Mechanistically, this improvement arises not only from increased photon flux but also from reduced background noise, due to the faster decomposition of trace phenol-dioxetane impurities.

Furthermore, stability studies confirmed that the incorporation of electronegative functionality into the adamantyl framework does not adversely affect probe integrity under physiological conditions, even over extended incubation

periods. This balance between reactivity and stability is critical for practical applications and highlights the effectiveness of our molecular design strategy. Overall, this work establishes electronegatively substituted adamantyl units as a powerful structural motif for next-generation chemiluminescent probes. The ability to simultaneously enhance chemiexcitation kinetics, detection sensitivity, and operational stability opens new opportunities for the development of advanced bioanalytical tools. We anticipate that this approach will be broadly applicable to diverse chemiluminescent systems and will facilitate the design of highly sensitive probes for diagnostic, imaging, and biological sensing applications.

Author contributions

T. L., N. N., D. W, and L. G. performed the synthesis and analyzed assay data under the supervision of D. S. J. I. performed the bacterial assays. All authors contributed to the discussion and writing of the manuscript.

Conflicts of interest

There are no conflicts to declare.

Data availability

The data supporting this article have been included as part of the supplementary information (SI). Supplementary information: includes synthetic procedures and characterization of all compounds, including 1H-NMR, 13C-NMR, HPLC, and MS, as well as experimental protocols and SI Figures. See DOI: https://doi.org/10.1039/d6sc03261c.

Acknowledgements

D.S. thanks the Israel Science Foundation (ISF) and the Binational Science Foundation (BSF) for financial support.

References

1 S. Gnaim and D. Shabat, *Acc. Chem. Res.*, 2019, **52**, 2806–2817.
2 N. Hananya and D. Shabat, *ACS Cent. Sci.*, 2019, **5**, 949–959.
3 U. Haris and A. R. Lippert, *ACS Sens.*, 2022, **8**, 3–11.
4 N. Hananya and D. Shabat, *Angew. Chem., Int. Ed.*, 2017, **56**, 16454–16463.
5 M. W. Yang, J. G. Huang, J. L. Fan, J. J. Du, K. Y. Pu and X. J. Peng, *Chem. Soc. Rev.*, 2020, **49**, 6800–6815.
6 S. Gnaim, O. Green and D. Shabat, *Chem. Commun.*, 2018, **54**, 2073–2085.
7 R. Blau, O. Shelef, D. Shabat and R. Satchi-Fainaro, *Nat Rev Bioeng.*, 2023, **1**, 648–664.
8 A. P. Schaap, T. S. Chen, R. S. Handley, R. Desilva and B. P. Giri, *Tetrahedron Lett.*, 1987, **28**, 1155–1158.
9 A. P. Schaap, R. S. Handley and B. P. Giri, *Tetrahedron Lett.*, 1987, **28**, 935–938.
10 A. P. Schaap, M. D. Sandison and R. S. Handley, *Tetrahedron Lett.*, 1987, **28**, 1159–1162.
11 O. Green, T. Eilon, N. Hananya, S. Gutkin, C. R. Bauer and D. Shabat, *ACS Cent. Sci.*, 2017, **3**, 349–358.
12 O. Green, S. Gnaim, R. Blau, A. Eldar-Boock, R. Satchi-Fainaro and D. Shabat, *J. Am. Chem. Soc.*, 2017, **139**, 13243–13248.
13 N. Hananya, O. Green, R. Blau, R. Satchi-Fainaro and D. Shabat, *Angew. Chem., Int. Ed.*, 2017, **56**, 11793–11796.
14 M. E. Roth-Konforti, C. R. Bauer and D. Shabat, *Angew. Chem., Int. Ed.*, 2017, **56**, 15633–15638.
15 K. J. Bruemmer, O. Green, T. A. Su, D. Shabat and C. J. Chang, *Angew. Chem., Int. Ed.*, 2018, **57**, 7508–7512.
16 N. Hananya, J. P. Reid, O. Green, M. S. Sigman and D. Shabat, *Chem. Sci.*, 2019, **10**, 1380–1385.
17 M. Roth-Konforti, O. Green, M. Hupfeld, L. Fieseler, N. Heinrich, J. Ihssen, R. Vorberg, L. Wick, U. Spitz and D. Shabat, *Angew. Chem., Int. Ed.*, 2019, **58**, 10361–10367.
18 S. Son, M. Won, O. Green, N. Hananya, A. Sharma, Y. Jeon, J. H. Kwak, J. L. Sessler, D. Shabat and J. S. Kim, *Angew. Chem., Int. Ed.*, 2019, **58**, 1739–1743.
19 S. Das, J. Ihssen, L. Wick, U. Spitz and D. Shabat, *Chem. Eur. J.*, 2020, **26**, 3647–3652.
20 S. Gutkin, O. Green, G. Raviv, D. Shabat and O. Portnoy, *Bioconjugate Chem.*, 2020, **31**, 2488–2493.
21 S. Ye, N. Hananya, O. Green, H. S. Chen, A. Q. Zhao, J. G. Shen, D. Shabat and D. Yang, *Angew. Chem., Int. Ed.*, 2020, **59**, 14326–14330.
22 S. P. Gholap, C. Y. Yao, O. Green, M. Babjak, P. Jakubec, T. Malatinsky, J. Ihssen, L. Wick, U. Spitz and D. Shabat, *Bioconjugate Chem.*, 2021, **32**, 991–1000.
23 S. Gutkin, S. Gandhesiri, A. Brik and D. Shabat, *Bioconjugate Chem.*, 2021, **32**, 2141–2147.
24 J. I. Scott, S. Gutkin, O. Green, E. J. Thompson, T. Kitamura, D. Shabat and M. Vendrell, *Angew. Chem., Int. Ed.*, 2021, **60**, 5699–5703.
25 O. Shelef, S. Gutkin, D. Feder, A. Ben-Bassat, M. Mandelboim, Y. Haitin, N. Ben-Tal, E. Bacharach and D. Shabat, *Chem. Sci.*, 2022, **13**, 12348–12357.
26 O. Shelef, T. Kopp, R. Tannous, M. Arutkin, M. Jospe-Kaufman, S. Reuveni, D. Shabat and M. Fridman, *J. Am. Chem. Soc.*, 2024, **146**, 5263–5273.
27 R. Tannous, O. Shelef, T. Kopp, M. Fridman and D. Shabat, *Bioconjugate Chem.*, 2024, **35**, 472–479.
28 M. David, S. Gutkin, R. V. Nithun, M. Jbara and D. Shabat, *Angew. Chem., Int. Ed.*, 2025, **64**, e202417924.
29 O. Shelef, S. Gutkin, M. Nassir, A. Krinsky, R. Satchi-Fainaro, P. S. Baran and D. Shabat, *Bioconjugate Chem.*, 2025, **36**, 152–159.
30 J. I. Scott, Z. M. Cheng, E. J. Thompson, U. Karmakar, V. Cowell, M. David, D. Gordon, L. Mendive-Tapia, A. Le Saint-Grant, P. Volkmer, C. S. Chuah, P. Lau, A. G. Rossi, W. B. Nagengast, D. Shabat, G. T. Ho and M. Vendrell, *Nat. Biomed. Eng.*, 2026, DOI: 10.1038/s41551-025-01588-1.
31 W. W. An, L. S. Ryan, A. G. Reeves, K. J. Bruemmer, L. Mouhaffel, J. L. Gerberich, A. Winters, R. P. Mason and A. R. Lippert, *Angew. Chem., Int. Ed.*, 2019, **58**, 1361–1365.

32 J. S. Huang, P. H. Cheng, C. Xu, S. S. Liew, S. S. He, Y. Zhang and K. Y. Pu, *Angew. Chem., Int. Ed.*, 2022, **61**, e202203235.
33 J. S. Huang, Y. Y. Jiang, J. C. Li, J. G. Huang and K. Y. Pu, *Angew. Chem., Int. Ed.*, 2021, **60**, 3999–4003.
34 H. N. Kagalwala, J. Gerberich, C. J. Smith, R. P. Mason and A. R. Lippert, *Angew. Chem., Int. Ed.*, 2022, **61**, e202210057.
35 X. Wei, J. S. Huang, C. Zhang, C. Xu, K. Y. Pu and Y. Zhang, *Angew. Chem., Int. Ed.*, 2023, **62**, e202213791.
36 J. Cao, W. W. An, A. G. Reeves and A. R. Lippert, *Chem. Sci.*, 2018, **9**, 2552–2558.
37 A. Acari, T. Almammadov, M. Dirak, G. Gulsoy and S. Kolemen, *J. Mater. Chem. B*, 2023, **11**, 6881–6888.
38 R. Tannous, O. Shelef, S. Gutkin, M. David, T. Leirikh, L. Ge, Q. Jaber, Q. Y. Zhou, P. C. Ma, M. Fridman, U. Spitz, K. N. Houk and D. Shabat, *ACS Cent. Sci.*, 2023, **10**, 28–42.
39 S. Gutkin, O. Shelef, Z. Babjaková, L. A. Tomanová, M. Babjak, T. Kopp, Q. Y. Zhou, P. C. Ma, M. Fridman, U. Spitz, K. N. Houk and D. Shabat, *JACS Au*, 2024, **4**, 3558–3566.
40 M. David, T. Leirikh, O. Shelef, S. Gutkin, T. Kopp, Q. Y. Zhou, P. C. Ma, M. Fridman, K. N. Houk and D. Shabat, *Angew. Chem., Int. Ed.*, 2024, **63**, e202410057.
41 O. Shelef, A. Krinsky, M. Jospe-Kaufman, Z. Babjaková, M. Fridman, R. Satchi-Fainaro, U. Spitz and D. Shabat, *Chem. Eur. J.*, 2024, **30**, e202402981.
42 M. David, T. Leirikh, N. Naama, T. Kopp and D. Shabat, *Angew. Chem., Int. Ed.*, 2025, **64**, e202515674.
43 R. Tannous, T. Kopp and D. Shabat, *JACS Au*, 2025, **5**, 2871–2883.